Published in final edited form as:
Cell Tissue Res. 2008 September ; 333(3): 427–438. doi:10.1007/s00441-008-0621-9.

Double gene deletion reveals the lack of cooperation between claudin 11 and claudin 14 tight junction proteins

Liron Elkouby-Naor[1], **Zaid Abassi**[2], **Ayala Lagziel**[3], **Alexander Gow**[4], and **Tamar Ben-Yosef**[1,*]

[1] Department of Genetics, The Rappaport Family Institute for Research in the Medical Sciences, Faculty of Medicine, Technion-Israel Institute of Technology, Haifa, Israel

[2] Department of Physiology and Biophysics, The Rappaport Family Institute for Research in the Medical Sciences, Faculty of Medicine, Technion-Israel Institute of Technology, Haifa, Israel

[3] Section on Human Genetics, Laboratory of Molecular Genetics, National Institute on Deafness and Other Communication Disorders, National Institutes of Health, Rockville, Maryland, USA

[4] Center for Molecular Medicine and Genetics, Carman and Ann Adams Department of Pediatrics, Department of Neurology, Wayne State University, Detroit, Michigan, USA

Summary

Members of the claudin family of proteins are the main components of tight junctions (TJs), the major selective barrier of the paracellular pathway between epithelial cells. Selectivity and specificity of TJ strands are determined by the type of claudins present. It is thus important to understand the cooperation between different claudins in various tissues. To study the possible cooperation between claudin 11 and claudin 14 we generated claudin11/claudin 14 double deficient mice. These mice exhibit a combination of the phenotypes found in each of the singly deficient mutants, including deafness, neurological deficits and male sterility. In the kidney we found that these two claudins have distinct and partially overlapping expression patterns. Claudin 11 is located in both the proximal and the distal convoluted tubules, while claudin 14 is located in both the thin descending and the thick ascending limbs of the loop of Henle, as well as in the proximal convoluted tubules. Although daily urinary excretion of Mg^{++}, and to a lesser extent of Ca^{++}, tended to be higher in claudin11/claudin 14 double mutants, these changes did not reach statistical significance comparing to wt animals. These findings suggest that under normal conditions co-deletion of claudin11 and claudin 14 does not affect kidney function or ion balance. Our data demonstrate that despite the importance of each of these claudins, there is probably no functional cooperation between them. Generation of additional mouse models in which different claudins are abolished will provide further insight into the complex interactions between claudin proteins in various physiological systems.

Keywords

tight junction; claudin 11; claudin 14; knockout mouse

Introduction

The transcellular and the paracellular routes are the pathways through which solutes and water move across epithelial cells and between them, respectively. The major selective barrier of the

[*]Correspondence to: Tamar Ben-Yosef, Department of Genetics, Rappaport Faculty of Medicine, Technion-Israel Institute of Technology, P.O. Box 9649, Bat Galim, Haifa 31096, Israel. Phone: 972-4-829-5228. Fax: 972-4-829-5225. benyosef@tx.technion.ac.il.

paracellular pathway is created by tight junctions (TJs). TJs form regions of intimate contact between the plasma membranes of adjacent epithelial cells (Farquhar and Palade 1963), thus preventing or reducing paracellular diffusion (Madara 1998). In addition to their barrier function TJs contribute to the maintenance of cellular polarity (Cereijido et al. 2000; Cereijido et al. 1998). Discoveries made in recent years revealed that TJs play important roles in various processes, including cell proliferation and differentiation, injury repair, immune response, drug delivery and cancer (Cereijido et al. 2007).

TJ strands are composed of at least four types of membrane-spanning proteins: occludin (Furuse et al. 1993), members of the junction adhesion molecule (JAM) family (Mandell and Parkos 2005), tricellulin (Ikenouchi et al. 2005; Riazuddin et al. 2006), and more than 20 members of the claudin family (Tsukita and Furuse 2000; Van Itallie and Anderson 2006). Important insight into the role of claudins came from the phenotypes of humans and animals with mutations in specific claudin genes. Mutations of human *CLDN1* underlie neonatal ichthyosis and sclerosing cholangitis (Hadj-Rabia et al. 2004). *Cldn1*-null mice and transgenic mice overexpressing *Cldn6* die shortly after birth due to dysfunction of the epidermal permeability barrier (Furuse et al. 2002; Turksen and Troy 2002). *Cldn5*-null mice die shortly after birth and show size-selective loosening of the blood-brain barrier (Nitta et al. 2003). *Cldn15*-null mice have megaintestine due to enhanced proliferation of normal cryptic cells after weaning (Tamura et al. 2008). *CLDN16*-deficiency leads to familial hypomagnesemia with hypercalciuria and nephrocalcinosis (FHHNC) in humans and mice, and to chronic interstitial nephritis in cattle (Hirano et al. 2000; Hou et al. 2007; Simon et al. 1999), due to dysfunction of paracellular renal transport mechanisms. Mutations of *CLDN19* in humans are associated with the combination of FHHNC and severe ocular involvement (Konrad et al. 2006). *Cldn19*-null mice present with peripheral nervous system deficits due to the absence of TJs from Schwann cells (Miyamoto et al. 2005). *Cldn11*-null mice demonstrate neurological and reproductive deficits, due to the absence of TJs in the central nervous system (CNS) myelin and between Sertoli cells in the testis (Gow et al. 1999). These mice also have hearing loss due to reduced endocochlear potentials (EP) (Gow et al. 2004; Kitajiri et al. 2004a). Mutations of human *CLDN14* cause profound, congenital deafness DFNB29 (Wilcox et al. 2001), and *Cldn14*-null mice are also deaf, due to rapid degeneration of cochlear outer hair cells (OHCs) shortly after birth (Ben-Yosef et al. 2003).

Claudins have various tissue distribution patterns, and most tissues express several different claudins (Furuse et al. 1999; Morita et al. 1999). Selectivity and specificity of paired TJ strands are determined by the type of claudins present and their stoichiometry (Furuse et al. 2001; Tsukita and Furuse 2000, 2002; Van Itallie and Anderson 2006). Within each organ different claudins may be part of the same heteropolymeric TJ strands or of separate TJ strands which interact with each other (Morita et al. 1999; Tsukita and Furuse 2000). In addition, different claudins may be located in separate segments within an organ. Segment-specific expression patterns of various claudins have been demonstrated in many organs, including the kidney (Kiuchi-Saishin et al. 2002; Reyes et al. 2002) and the inner ear (Kitajiri et al. 2004b).

A useful approach for studying the interactions between different claudins and their possible synergistic effects is to create mouse models in which more than one claudin is abolished. Six claudin mouse knockouts have been reported to date (Ben-Yosef et al. 2003; Furuse et al. 2002; Gow et al. 1999; Miyamoto et al. 2005; Nitta et al. 2003; Tamura et al. 2008). We chose two of these knockout strains (*Cldn11*- and *Cldn14*-null mice) and generated claudin11/claudin 14 double mutants. We carefully evaluated these mice to study the organ systems already affected in each of the strains, as well as other systems expressing both *Cldn11* and *Cldn14*.

Materials and methods

All experiments were performed according to the guidelines of the committee for the supervision of animal experiments, Technion- Israel Institute of Technology.

DNA and RNA analysis

Extraction of genomic DNA from mouse tails was performed with the High Pure PCR Template Preparation Kit (Roche). Genotype of *Cldn11* was determined by a PCR-based assay as described previously (Gow et al. 1999) (Fig. 1b). Genotype of *Cldn14* was determined by a PCR-based assay, as follows: The wild type (wt) allele was amplified with a common primer (GGC TGCATAACCAGGATACTC) and a wt primer (GTACAGGCTGAATGACTACGTG) (340bp product). The knockout allele was amplified with the common primer and a mutant primer (CAGCTCATTCCTCCCACTCATGAT C) (275bp product) (Fig. 1b). Cycling conditions were 95°C for one minute, followed by 35 cycles of 95°C for 30 seconds, 55°C for 30 seconds, and 72°C for 30 seconds, and a final step of 72 °C for ten minutes.

Total RNA was isolated from mouse organs using Tri reagent (sigma), and treated with RQ1 RNase-free DNase (promega). Reverse transcription was performed with 1 μg of total RNA in a 20-μl reaction volume using Superscript II reverse transcriptase (Invitrogen). RT-PCR was performed with 2 μl of cDNA in a 50-μl reaction volume in the presence of 1X PCR reaction buffer, 0.02 U of thermostable DNA polymerase (gene choice), 20 pmol each of forward and reverse primers, 100 mM of each dNTP, and 1.5 mM $MgCl_2$. Primer sequences and cycling conditions for *Cldn14* and *Actb* were reported previously (Ben-Yosef et al. 2003). Primer sequences for *Cldn11* were: TGAGTCGAGCTGCGTGGACGTC and CGTACAGCGAGTAGCCAAAGC. Cycling conditions were 95°C for one minute, followed by 35 cycles of 95°C for 30 seconds, 60°C for 30 seconds, and 72°C for 60 seconds, and a final step of 72°C for 10 minutes.

Relative expression levels of claudin family members in kidney and inner ear were analyzed by semi-quantitative RT-PCR. cDNA was subjected to PCR amplification with primer-pairs specific to each claudin, under non-saturating conditions (21–32 cycles of amplification). Primer sequences were as follows: *Cldn1*: TTGCAGAGACCCCATCACCTTCGC and CTGTTTCCATACCATGCTGTGGC; *Cldn19*: CTGAGTCCTGGAACTCTCAGAC and CAGACGTACTCTCTGGCAGCAG; *Cldn23*: ACCTCGCAGATTCGAGGACAG and GCCAGTGACGTGATCATGAGTC; *Cldn2* and *Cldn7* (Yi et al. 2000); *Cldn3*, *Cldn4*, *Cldn5*, *Cldn8*, *Cldn10*, *Cldn12*, *Cldn13*, *Cldn15*, *Cldn16* (Acharya et al. 2004); *Cldn6* (Turksen and Troy 2002). PCR products were subjected to electrophoresis on a 10% acrylamide gel and relative band intensities were quantified with ImageMaster (Bio-Rad) and TotalLab (Phoretix International) software. Results were normalized based on relative expression levels of β-actin (*Actb*) in each sample.

Histology

Cochleae were obtained from mice of each genotype (wt, *Cldn14*, $Cldn11^{-/-}$ and $Cldn11^{-/-}$/$Cldn14^{-/-}$) at the age of two months. Cochleae were decalcified by incubation in a 4% paraformaldehyde/100 mM EDTA solution at 4°C for three days with continuous shaking, embedded in paraffin, sectioned at 8 μm, and stained with hematoxylin and eosin.

Serum and urine chemical analysis

Serum and urine were collected from seven mice of each genotype (wt and $Cldn11^{-/-}$/$Cldn14^{-/-}$) at three to four months of age. Mice were fed standard rodent chow containing 0.23% Na^+, 0.2% Mg^{++}, 1.01% Ca^{++}, and 0.68% K^+ (Harlan Teklad), and tap water *ad*

libitum. The animals were kept in individual metabolic cages in a temperature-controlled room, for one week to obtain baseline values of urinary creatinine, protein, Ca^{++}, Mg^{++}, K^{+}, and Na^{+} excretion. During this period, mean arterial blood pressure (MAP) was measured using a tail-cuff method (IITC, model 31) after maintaining the animals in an incubator at 37°C for 15 minutes to ensure vasodilatation. For each mouse, MAP was measured at least three times. On day 8 the mice were sacrificed, and blood samples were collected for chemical analysis of Ca^{++}, Mg^{++}, K^{+}, Na^{+}, and creatinine (Biochemical Laboratories, Rambam Medical Center).

Auditory and neurologic testing

Neurologic function of six mice of each genotype (wt, *Cldn14*$^{-/-}$, *Cldn11*$^{-/-}$ and *Cldn11*$^{-/-}$/*Cldn14*$^{-/-}$) was evaluated at the age of three months by a beam-walking test, following standard procedures (Carter et al. 1997). Hearing was evaluated by Auditory Brainstem Response (ABR) analysis using an auditory evoked potential diagnostic system (Intelligent Hearing Systems) with high-frequency transducers, as previously described (Ben-Yosef et al. 2003). Analysis was performed on five to eleven mice of each genotype (wt, *Cldn14*$^{-/-}$, *Cldn11*$^{-/-}$ and *Cldn11*$^{-/-}$/*Cldn14*$^{-/-}$) at two months of age. The maximum sound intensities tested were 100 dB-SPL for 8 and 32 kHz, and 90 dB-SPL for 16kHz.

Immunohistochemistry

Inner ears of wt, *Cldn14*$^{-/-}$, *Cldn11*$^{-/-}$ and *Cldn11*$^{-/-}$/*Cldn14*$^{-/-}$ mice at postnatal day 16 (P16) were dissected from temporal bones and fixed in 4% paraformaldehyde in PBS for 2 hours. The organ of Corti was processed for immunohistochemistry as previously described (Belyantseva et al. 2003). Immunohistochemistry was performed with a specific antibody raised against a peptide (CTASLPQEDMEPNATPTTPEA) located within the C-terminus of mouse prestin. F-actin was visualized by rhodamine phalloidinstaining (Molecular Probes) as previously described (Beyer et al. 2000).

To determine the localization of claudin 11 and claudin 14 within the kidney, the following markers for various nephron segments were used: aquaporin-1 (AQP1) (proximal convoluted tubules in the cortex and thin descending limb of the loop of Henle in the medulla); aquaporin-2 (AQP2) (collecting ducts); Tamm-Horsfall glycoprotein (THP) (thick ascending limb of the loop of Henle); and cytokeratin K8 (CK8) (collecting ducts, distal convoluted tubules in the cortex, and thin ascending limb of the loop of Henle in the medulla) (Kiuchi-Saishin et al. 2002; Piepenhagen et al. 1995). Kidneys were removed from wt male mice (three months old), frozen with liquid nitrogen, sectioned with a cryostat, mounted on single glass slides, and air-dried. Sections were then fixed with 95% ethanol at 4 °C for 30 min, followed by 100% acetone at room temperature for 1 min. After incubating with 0.2% triton X-100 for 10 min and soaking in PBS containing 1% bovine serum albumin, sections were incubated for 60 min in a moist chamber with rabbit anti-claudin 14 (Wilcox et al. 2001), rabbit anti-claudin 11 (Zymed Laboratories), chicken anti-CK8 (Abcam), goat anti-THP, goat anti-AQP1, or goat anti-AQP2 (Santa Cruz Biotechnology) as primary antibodies (pAb). Sections were then washed three times with PBS, followed by 60 min incubation with the appropriate secondary antibodies. Secondary antibodies used were FITC-conjugated donkey anti-rabbit IgG (Amersham Biosciences), Cy3-conjugated donkey anti-goat IgG, Cy3-conjugated goat anti-rabbit IgG, and Cy2-conjugated goat anti-chicken IgG (Jackson ImmunoResearch Laboratories). After being washed with PBS, sections were embedded with Vectashield containing DAPI (Vector Laboratories). Slides were viewed with a BioRad confocal microscope.

Results

Generation of claudin 11/claudin 14 double knockout mice

Claudin 11- and claudin 14-singly deficient mice were generated and characterized previously (Ben-Yosef et al. 2003; Gow et al. 1999). The mating scheme for generating claudin11/claudin 14 double mutants is described in Figure 1a. Double mutants were obtained by three consecutive generations of matings. In the third generation, *Cldn11*$^{-/-}$/*Cldn14*$^{-/-}$ mice constituted 25% of the offspring, as expected (Fig. 1a). Genotypes were confirmed by PCR-based assays (Fig. 1b). No *Cldn11* or *Cldn14* transcripts were detected by RT-PCR from brains of *Cldn11*$^{-/-}$/*Cldn14*$^{-/-}$ mice (Fig. 1c). Claudin 11/claudin 14 double mutants are viable and exhibit normal growth, thus demonstrating that elimination of both these TJ proteins is compatible with life.

Reproductive and neurological deficits in claudin 11/claudin 14 double mutants

Cldn14-null mice are fertile and have normal neurological function (Ben-Yosef et al. 2003). *Cldn11*-null mice have neurological abnormalities, mainly presenting as hindlimb weakness, which is attributed to the lack of TJs in the CNS myelin. In addition, *Cldn11*-null males are sterile, due to the absence of TJs from between Sertoli cells in the testis (Gow et al. 1999). As expected, claudin 11/claudin 14 double mutant males are also sterile. In addition, both males and females exhibit hindlimb weakness similar to claudin 11-deficient mice.

Hearing loss with normal vestibular function in claudin 11/claudin 14 double mutants

Both *Cldn11* and *Cldn14* are expressed in the inner ear. However, within this organ their expression is confined to separate compartments. *Cldn11* is mainly expressed in basal cells of the stria vascularis (St.V.), while *Cldn14* is expressed in inner and outer hair cells (IHCs and OHCs) and in supporting cells in the organ of Corti. Low expression levels of both genes were reported in other sections of the inner ear, including the vestibular sensory epithelium (Ben-Yosef et al. 2003; Gow et al. 2004; Gow et al. 1999; Kitajiri et al. 2004a; Kitajiri et al. 2004b). However, no vestibular abnormalities were found in claudin 14-deficient humans and mice, or in claudin 11-deficient mice (Ben-Yosef et al. 2003; Gow et al. 1999; Wilcox et al. 2001). We made the same observation in claudin 11/claudin 14 double mutants, which display no obvious abnormal behavior indicative of vestibular dysfunction in mice, such as circling, head tossing or hyperactivity.

Both *Cld11*- and *Cldn14*-null mice have severe hearing loss at all frequencies tested (Ben-Yosef et al. 2003; Gow et al. 2004; Kitajiri et al. 2004a). At the age of two months *Cldn14*-null mice have hearing loss of over 40 dB-SPL at the low frequencies (8 and 16 kHz), and approximately 30 dB-SPL at the high frequencies (32kHz), in comparison to wt littermates. At the same age hearing loss in *Cldn11*-null mice appears to be milder (22–27 dB-SPL over all frequencies tested), although the difference is not statistically significant (Table 1). At two months of age claudin 11/claudin 14 double mutants were found to have ABR thresholds similar to those obtained from *Cldn14*-null mice at the same age (Table 1).

Cochlear pathology in claudin 11/claudin 14 double mutants

Inner ears of *Cldn14*-nullmice develop normally and both IHCs and OHCs are present and undistinguishable from wt mice at P7. However, subsequently rapid loss of OHCs is observed, which is followed by loss of IHCs (Ben-Yosef et al. 2003) (Fig. 2). *Cldn11*-null mice have normal and functional IHCs and OHCs. However, in these mice TJs between basal cells of the St.V. are missing. No gross morphological malformations are observed in inner ears of *Cldn11*-nullmice, except for an edematous appearance of the St.V., which may reflect changes in ion composition of the intrastrial space, caused by infusion of perilymph from surrounding

regions (Gow et al. 2004; Kitajiri et al. 2004a) (Fig. 2a). Histological analysis of inner ear sections of claudin11/claudin 14 double mutants at the age of two months revealed a combination of hair cell loss at the organ of Corti, and an edematous appearance of the St.V. (Fig. 2a). No additional abnormalities were observed. The timing of OHC loss in claudin11/claudin 14 double mutants is similar to *Cldn14*-nullmice, as by P16 most OHCs are missing throughout the cochlea in mice of both genotypes (Fig. 2b).

Claudin 11/Claudin 14 double knockout mice have normal kidney function

Both *Cldn11* and *Cldn14* are highly expressed in kidney, yet no renal dysfunction was observed in humans and mice homozygous for *CLDN14* mutations (Ben-Yosef et al. 2003; Wilcox et al. 2001), or in *Cldn11*- null mice (Gow et al. 1999). Within the kidney we found that claudin 11 is mainly expressed in the cortex, where it partially co-localizes with AQP1 and fully co-localizes with CK8 (Fig. 3), but not with AQP2 (data not shown). These findings indicate that claudin 11 is located in both the proximal and the distal convoluted tubules, but not in the collecting duct. Claudin 11 was also reported to co-localize with THP in the thick ascending limb of the loop of Henle (Kiuchi-Saishin et al. 2002). However, we did not find such co-localization. The reason for these different observations is unclear, but may result from differences in antibody specificities.

We have previously found high expression levels of *Cldn14* in the kidney medulla, based on X-gal staining (Ben-Yosef et al. 2003). Following immunostaining of mouse kidney sections with an antibody against claudin 14 we observed that claudin 14 was expressed in both medulla and cortex, although staining in the cortex was less intense. Co-immunostaining with antibodies against claudin 14 and markers for various nephron segments revealed co-localization of claudin 14 with AQP1 in both medulla and cortex. In addition, claudin 14 co-localized with THP in the medulla (Fig. 3). These findings indicate that claudin 14 is located in both the thin descending and the thick ascending limbs of the loop of Henle, as well as in the proximal convoluted tubules.

Our data indicate that claudin 11 and claudin 14 have distinct and partially overlapping expression patterns in the nephron. Both claudins are located in the proximal convoluted tubules, but only the later is expressed in Henles' loop. In order to evaluate the physiological relevance of *Cldn11/Cldn14* double gene deletion, we performed a panel of tests including plasma and urine chemical analysis and measurement of glomerular filtration rate (GFR) and blood pressure in claudin11/claudin 14 double mutants and wt animals. Selected renal and systemic characteristics of the two groups of animals are depicted in Table 2. There were no significant differences in plasma concentrations of Ca^{++}, Mg^{++}, Na^{+}, K^{+}, and creatinine between the two groups. In addition, kidney function, expressed as GFR, kidney weight, and blood pressure were comparable in claudin11/claudin 14 double mutants and their wt littermates. While urinary Ca^{++} excretion increased by ~20% in claudin 11/claudin 14 double mutants, urinary Mg^{++} was enhanced by ~71%. Although daily urinary excretion of Mg^{++}, and to a lesser extent of Ca^{++}, tended to be higher in claudin11/claudin 14 double mutant mice, these changes did not reach statistical significance when compared to wt animals. These findings suggest that co-deletion of claudin11 and claudin 14 does not affect kidney function or Mg^{++} and Ca^{++} balance, at least under normal conditions.

Expression levels of claudin genes in kidneys and inner ears of *Cldn11*/*Cldn14* double mutant mice

At least ten distinct claudins are expressed in various segments of the inner ear (Kitajiri et al. 2004b) and at least 15 are expressed in the adult mouse kidney (Angelow et al. 2007; Ben-Yosef et al. 2003; Kiuchi-Saishin et al. 2002; Li et al. 2004). A possible mechanism for maintaining homeostasis within a TJ strand may involve tight co-regulation of different

claudins. Therefore, alteration of one or more claudin may have regulatory repercussions on other claudins expressed in the same tissue. To test this hypothesis we used semi-quantitative RT-PCR to analyze the expression levels of various claudin genes in kidneys and inner ears from wt and *Cldn11*$^{-/-}$*Cldn14*$^{-/-}$ mice. Only a two-fold increase or higher was considered significant. Our analysis revealed that in the ear the simultaneous elimination of both *Cldn11* and *Cldn14* did not lead to a compensatory up-regulation of other types of claudins (Fig. 4a). In the kidney, four claudin genes (*Cldn3*, *Cldn5*, *Cldn7*, and *Cldn23*) were slightly up-regulated (2.2–2.5 fold increase in expression level) in the double mutants, in comparison to wt mice (Fig. 4b).

Discussion

TJs play a central role in the regulation of paracellular permeability. Members of the claudin family contribute to the structure of TJs in a variety of tissue types. Particular combinations and quantities of claudins modulate the charge selective permeability of the paracellular pathway and, hence, take part in the regulation of the ionic makeup of extracellular fluids (Van Itallie and Anderson 2006). Claudins have various tissue distribution patterns. Some claudins are restricted to specific cell types (e.g. claudin 16 in the thick ascending limb of the loop of Henle) (Simon et al. 1999), and some tissues express a single claudin (e.g. claudin 11 in CNS oligodendrocytes and in Sertoli cells) (Gow et al. 1999). Yet, most tissues express several different claudins and most claudins are expressed in more than one tissue (Furuse et al. 1999; Morita et al. 1999; Van Itallie and Anderson 2006).

Elimination of a certain claudin can have various effects on TJ structure and function. For example, the elimination of claudin 11 leads to complete absence of TJ strands in certain regions of the CNS, testes and inner ear (Gow et al. 2004; Gow et al. 1999; Kitajiri et al. 2004a). On the other hand, in the absence of claudin 14 TJ strands between hair cells and supporting cells in the organ of Corti are present and appear normal, but TJ function is severely altered (Ben-Yosef et al. 2003). Elimination of either claudin 11 or claudin 14 does not have an apparent effect on TJ function in the kidney (Gow et al. 2004; Gow et al. 1999; Kitajiri et al. 2004a). These findings further demonstrate that the combination and stoichiometry of claudins in a TJ are important, but that other factors (such as other TJ proteins) are also involved in generation and maintenance of TJ structure and/or function in certain epithelial tissues.

To date six claudin mouse knockouts have been generated (*Cldn1*-, *Cldn5*-, *Cldn15*-, *Cldn19*-, *Cldn11*- and *Cldn14-null* mice), but a claudin double mutant has not yet been reported. We generated claudin 11/claudin 14 double mutants and evaluated them to study the organ systems already affected in each of the singly deficient strains (mainly the inner ear), as well as other organs expressing both *Cldn11* and *Cldn14* (*i.e.*, kidney). Our hypothesis was that if one of these two claudins can substitute for the other, then in the absence of both claudins, a new defect might emerge, which is not elicited by the absence of each claudin separately. However, claudin 11/claudin 14 double mutants were found to exhibit a combination of the phenotypes found in each of the singly deficient strains, and no additional phenotypes were detected.

At least ten distinct claudins are expressed in various segments of the inner ear (Kitajiri et al. 2004b). Only two of them, claudin 11 and claudin 14, have been associated with hearing loss. However, the spatial expression patterns of *Cldn11* and *Cldn14* within the inner ear and the etiology of inner ear dysfunction caused by mutations of each of these claudins are different. *Cldn11* is expressed in basal cells of the St.V., while *Cldn14* is expressed in IHCs and OHCs and in supporting cells within the organ of Corti. . In *Cldn14*-null mice by the age of three weeks nearly all OHCs are lost, and there is a partial loss of IHCs as well. In mammals, OHCs are electromechanical cochlear amplifiers which enhance hearing sensitivity by more than 40 dB (Dallos and Harris 1978; Ryan and Dallos 1975). Indeed, a hearing loss of 40 dB or more

is found in these mice as early as P15 (Ben-Yosef et al. 2003). We assumed that the process of OHC loss in *Cldn14*-null mice was due to an altered ionic composition within the space of Nuel, which surrounds the basolateral membranes of OHCs. Specifically, we have previously demonstrated that claudin 14 is highly selective against cations. These properties are precisely what would be required to maintain the high cation gradients between perilymph and endolymph. Presumably, in the absence of claudin 14 the ability to maintain the paracellular barrier against cations at the reticular lamina is lost, and perhaps results in elevated K^+ concentration in the space of Nuel. This environment is probably toxic to the basolateral membrane of OHCs (Ben-Yosef et al. 2003).

The cause for hearing loss in *Cldn11*-null mice is reduced EP. The electrogenic machinery that generates the EP is localized in the St.V. (Salt et al. 1987). In *Cldn11*-null mice the absence of a paracellular barrier between basal cells of the St.V. renders the intrastrial space open to perilymph, and abolishes its electrical isolation (Gow et al. 2004; Gow et al. 1999; Kitajiri et al. 2004a).

Since *Cldn11* and *Cldn14* expression patterns within the inner ear do not overlap, physical interaction between them within the TJ strand is not possible. Yet, we hypothesized that they could cooperate through their effects on inner ear ion balance and homeostasis. Hypothetically, reduction of endolymphatic K^+ concentration due to the lack of claudin 11 could prevent the OHC degeneration that is caused by the lack of claudin 14. Nevertheless, such double-deficient mice would still be deaf, due to reduced EP. In fact, inner ear pathology in *Cldn11/Cldn14* double mutants involves both loosening of the intrastrial compartment and rapid degeneration of OHCs, which happens at the same timing as in *Cldn14*-null mice (Fig. 2). This finding indirectly indicates that in *Cldn11/Cldn14* double mutants, like in *Cldn11*-singly deficient mice, despite the marked reduction in EP, the absence of basal cell TJs appears to cause minimal disruption to ion homeostasis in the cochlea, as K^+ levels in endolymph of *Cldn11*-null mice are normal (Gow et al. 2004;Kitajiri et al. 2004a).

Of the 24 claudins annotated in mammalian genomes, at least 15 are expressed in the adult mouse kidney (Angelow et al. 2007; Ben-Yosef et al. 2003; Kiuchi-Saishin et al. 2002; Li et al. 2004). In every segment of the kidney nephron several claudins are expressed simultaneously (Kiuchi-Saishin et al. 2002). For example, at least five distinct claudins are located in the thick ascending limb of the loop of Henle. These include claudins 3, −10, −14, −16 and −19 (Angelow et al. 2007; Kiuchi-Saishin et al. 2002) (Fig. 3). Such expression pattern may lead to marked redundancy between claudins, and serve as a backup mechanism. Nevertheless, mutations of either claudin 16 or claudin 19 have been associated with a severe renal phenotype (FHHNC) (Hirano et al. 2000; Hou et al. 2007; Konrad et al. 2006; Simon et al. 1999). On the other hand, claudin 14-deficiency has no obvious effect on kidney function (Ben-Yosef et al. 2003; Wilcox et al. 2001). Taken together, these observations demonstrate that in certain tissues some claudins appear to be indispensable, while others appear to be functionally redundant. However, it is possible that the combined loss of two or more “nonessential” claudins will elicit an abnormal phenotype.

Our data indicate that the segment-specific expression patterns of claudin 11 and claudin 14 in kidney nephrons are partially overlapping, since both of them (as well as claudins 1, −2, −10 and −12) are located in the adult mouse proximal convoluted tubules (Fig. 3) (Abuazza et al. 2006;Kiuchi-Saishin et al. 2002). It has been shown that claudins determine epithelial ion permeability through the electrostatic charges of specific amino acid residues on their first extracellular loops (Colegio et al. 2003). For example, claudins 2 and −15 are cation-selective. In contrast, both claudin 11 and claudin 14 are anion-selective (discriminative against cations) (Ben-Yosef et al. 2003;Van Itallie et al. 2003). Based on these similar electrophysiological properties, one may assume that claudin 11 and claudin 14 are compatible in the nephron, and

that simultaneous elimination of both claudins would affect renal handling of certain electrolytes. Yet, no significant kidney dysfunction or electrolyte disturbance were observed in *Cldn11/Cldn14* double mutant mice. The co-expression of claudin 11 and claudin 14 in the proximal tubules supports our findings, since in this segment of the nephron the majority of filtered electrolytes are reabsorbed via the transcellular, rather than via the paracellular route (Dantzler 2003;Hebert 1999;Naderi and Reilly 2008). The elimination of claudin 14, which we found to be expressed in Henle's loop, where two thirds of the filtered Mg^{++} and a quarter of the filtered Ca^{++} are paracellularly reabsorbed, may contribute to the observed mild enhancement in Mg^{++} and Ca^{++} excretion in *Cldn11/Cldn14* double mutant mice. However, further studies are required to determine whether and to which extent claudin 14 is involved in Mg^{++} and Ca^{++} homeostasis, as compared with the well-established role of claudin 16 and claudin 19 in this process (Naderi and Reilly 2008).

While analyzing the phenotype of *Cldn11/Cldn14* double mutants, one must consider the possibility that simultaneous elimination of both claudins may have regulatory repercussions on other claudins, and affect the final outcome. Our analysis indicates that this is not the case in the inner ear, where no significant increase in expression levels of various claudin genes was observed (Fig. 4a). In the kidney, a mild increase was observed in expression levels of *Cldn3*, *Cldn5*, *Cldn7*, and *Cldn23* (Fig. 4b). *Cldn5* is expressed only in endothelial cells of blood vessels (Kiuchi-Saishin et al. 2002), and thus its relevance to kidney function in the double mutants is unclear. *Cldn3* is expressed in Henle's loop, in distal convoluted tubules, and in collecting ducts (Kiuchi-Saishin et al. 2002). The location of *Cldn7* and *Cldn23* expression within the mouse nephron is unknown. It cannot be ruled out that increased expression levels of these genes in the double mutants represent a compensatory up-regulation. Nevertheless, their effect on the renal phenotype remains to be determined.

On one hand, our results further demonstrate the marked redundancy between claudins in the kidney. On the other hand, they raise questions regarding the biological basis for expressing such a wide repertoire of claudin family members in the kidney, given that at least some of them do not appear to be essential for normal renal function, and that even the combined elimination of two claudins is well tolerated by this organ, as described here. It is possible that some claudins become important under certain types of physiological stress, but not under normal conditions. From an evolutionary point of view, another possibility is that the variety of claudins expressed in the kidney (and in other organs) is under a constant process of fine-tuning, and the fact that certain family members are expressed in the kidney at this point in time does not necessarily reflect an essential role in renal function.

In summary, *Cldn11/Cldn14* double mutant mice exhibit a combination of the phenotypes found in each of the singly deficient mutants, but no additional abnormalities. While it cannot be said with certainty that claudin 11 and claudin 14 are not cooperative based on these findings alone, our data do not support such hypothetical cooperation. Generation of additional mouse models in which different claudin combinations are abolished will provide further insight into the complex interactions between claudin family members in various physiological systems.

Acknowledgments

We thank Thomas Friedman for anti-prestin and anti-claudin 14 antibodies, Karen Avraham for the use of her ABR system, Hoda Awad for technical assistance, and Thomas Friedman and James Anderson for critical reading of this manuscript.

Grant information: This work was supported by the Israel Science Foundation (grant number 24/05) and by NIDCD/NIH intramural research funds (Z01-DC-00039-11).

References

Abuazza G, Becker A, Williams SS, Chakravarty S, Truong HT, Lin F, Baum M. Claudins 6, 9, and 13 are developmentally expressed renal tight junction proteins. Am J Physiol Renal Physiol 2006;291:F1132–1141. [PubMed: 16774906]

Acharya P, Beckel J, Ruiz WG, Wang E, Rojas R, Birder L, Apodaca G. Distribution of the tight junction proteins ZO-1, occludin, and claudin-4, -8, and -12 in bladder epithelium. Am J Physiol Renal Physiol 2004;287:F305–318. [PubMed: 15068973]

Angelow S, El-Husseini R, Kanzawa SA, Yu AS. Renal localization and function of the tight junction protein, claudin-19. Am J Physiol Renal Physiol 2007;293:F166–177. [PubMed: 17389678]

Belyantseva IA, Boger ET, Friedman TB. Myosin XVa localizes to the tips of inner ear sensory cell stereocilia and is essential for staircase formation of the hair bundle. Proc Natl Acad Sci U S A 2003;100:13958–13963. [PubMed: 14610277]

Ben-Yosef T, Belyantseva IA, Saunders TL, Hughes ED, Kawamoto K, Van Itallie CM, Beyer LA, Halsey K, Gardner DJ, Wilcox ER, Rasmussen J, Anderson JM, Dolan DF, Forge A, Raphael Y, Camper SA, Friedman TB. Claudin 14 knockout mice, a model for autosomal recessive deafness DFNB29, are deaf due to cochlear hair cell degeneration. Hum Mol Genet 2003;12:2049–2061. [PubMed: 12913076]

Beyer LA, Odeh H, Probst FJ, Lambert EH, Dolan DF, Camper SA, Kohrman DC, Raphael Y. Hair cells in the inner ear of the pirouette and shaker 2 mutant mice. J Neurocytol 2000;29:227–240. [PubMed: 11276175]

Carter, J.; Morton, JA.; Dunnet, SB. Motor coordination and balance in rodents. In: Crawley, JC.; Rogawski, MA.; Sibley, DR.; Skolnik, P.; Wray, S., editors. Current protocols in neuroscience. Vol. 2. John Wiley and Sons, Inc; New York: 1997. p. 8.12.11-18.12.14.

Cereijido M, Contreras RG, Flores-Benitez D, Flores-Maldonado C, Larre I, Ruiz A, Shoshani L. New diseases derived or associated with the tight junction. Arch Med Res 2007;38:465–478. [PubMed: 17560451]

Cereijido M, Shoshani L, Contreras RG. Molecular physiology and pathophysiology of tight junctions. I. Biogenesis of tight junctions and epithelial polarity. Am J Physiol Gastrointest Liver Physiol 2000;279:G477–482. [PubMed: 10960345]

Cereijido M, Valdes J, Shoshani L, Contreras RG. Role of tight junctions in establishing and maintaining cell polarity. Annu Rev Physiol 1998;60:161–177. [PubMed: 9558459]

Colegio OR, Van Itallie C, Rahner C, Anderson JM. Claudin extracellular domains determine paracellular charge selectivity and resistance but not tight junction fibril architecture. Am J Physiol Cell Physiol 2003;284:C1346–1354. [PubMed: 12700140]

Dallos P, Harris D. Properties of auditory nerve responses in absence of outer hair cells. J Neurophysiol 1978;41:365–383. [PubMed: 650272]

Dantzler WH. Regulation of renal proximal and distal tubule transport: sodium, chloride and organic anions. Comp Biochem Physiol A Mol Integr Physiol 2003;136:453–478. [PubMed: 14613778]

Farquhar MG, Palade GE. Junctional complexes in various epithelia. J Cell Biol 1963;17:375–412. [PubMed: 13944428]

Furuse M, Furuse K, Sasaki H, Tsukita S. Conversion of zonulae occludentes from tight to leaky strand type by introducing claudin-2 into Madin-Darby canine kidney I cells. J Cell Biol 2001;153:263–272. [PubMed: 11309408]

Furuse M, Hata M, Furuse K, Yoshida Y, Haratake A, Sugitani Y, Noda T, Kubo A, Tsukita S. Claudin-based tight junctions are crucial for the mammalian epidermal barrier: a lesson from claudin-1-deficient mice. J Cell Biol 2002;156:1099–1111. [PubMed: 11889141]

Furuse M, Hirase T, Itoh M, Nagafuchi A, Yonemura S, Tsukita S, Tsukita S. Occludin: a novel integral membrane protein localizing at tight junctions. J Cell Biol 1993;123:1777–1788. [PubMed: 8276896]

Furuse M, Sasaki H, Tsukita S. Manner of interaction of heterogeneous claudin species within and between tight junction strands. J Cell Biol 1999;147:891–903. [PubMed: 10562289]

Gow A, Davies C, Southwood CM, Frolenkov G, Chrustowski M, Ng L, Yamauchi D, Marcus DC, Kachar B. Deafness in Claudin 11-null mice reveals the critical contribution of basal cell tight junctions to stria vascularis function. J Neurosci 2004;24:7051–7062. [PubMed: 15306639]

Gow A, Southwood CM, Li JS, Pariali M, Riordan GP, Brodie SE, Danias J, Bronstein JM, Kachar B, Lazzarini RA. CNS myelin and sertoli cell tight junction strands are absent in Osp/claudin-11 null mice. Cell 1999;99:649–659. [PubMed: 10612400]

Hadj-Rabia S, Baala L, Vabres P, Hamel-Teillac D, Jacquemin E, Fabre M, Lyonnet S, De Prost Y, Munnich A, Hadchouel M, Smahi A. Claudin-1 gene mutations in neonatal sclerosing cholangitis associated with ichthyosis: a tight junction disease. Gastroenterology 2004;127:1386–1390. [PubMed: 15521008]

Hebert SC. Molecular mechanisms. Semin Nephrol 1999;19:504–523. [PubMed: 10598539]

Hirano T, Kobayashi N, Itoh T, Takasuga A, Nakamaru T, Hirotsune S, Sugimoto Y. Null mutation of PCLN-1/Claudin-16 results in bovine chronic interstitial nephritis. Genome Res 2000;10:659–663. [PubMed: 10810088]

Hou J, Shan Q, Wang T, Gomes AS, Yan Q, Paul DL, Bleich M, Goodenough DA. Transgenic RNAi depletion of claudin-16 and the renal handling of magnesium. J Biol Chem. 2007

Ikenouchi J, Furuse M, Furuse K, Sasaki H, Tsukita S, Tsukita S. Tricellulin constitutes a novel barrier at tricellular contacts of epithelial cells. J Cell Biol 2005;171:939–945. [PubMed: 16365161]

Kitajiri S, Miyamoto T, Mineharu A, Sonoda N, Furuse K, Hata M, Sasaki H, Mori Y, Kubota T, Ito J, Furuse M, Tsukita S. Compartmentalization established by claudin-11-based tight junctions in stria vascularis is required for hearing through generation of endocochlear potential. J Cell Sci 2004a; 117:5087–5096. [PubMed: 15456848]

Kitajiri SI, Furuse M, Morita K, Saishin-Kiuchi Y, Kido H, Ito J, Tsukita S. Expression patterns of claudins, tight junction adhesion molecules, in the inner ear. Hear Res 2004b;187:25–34. [PubMed: 14698084]

Kiuchi-Saishin Y, Gotoh S, Furuse M, Takasuga A, Tano Y, Tsukita S. Differential expression patterns of claudins, tight junction membrane proteins, in mouse nephron segments. J Am Soc Nephrol 2002;13:875–886. [PubMed: 11912246]

Konrad M, Schaller A, Seelow D, Pandey AV, Waldegger S, Lesslauer A, Vitzthum H, Suzuki Y, Luk JM, Becker C, Schlingmann KP, Schmid M, Rodriguez-Soriano J, Ariceta G, Cano F, Enriquez R, Juppner H, Bakkaloglu SA, Hediger MA, Gallati S, Neuhauss SC, Nurnberg P, Weber S. Mutations in the tight-junction gene claudin 19 (CLDN19) are associated with renal magnesium wasting, renal failure, and severe ocular involvement. Am J Hum Genet 2006;79:949–957. [PubMed: 17033971]

Li WY, Huey CL, Yu AS. Expression of claudin-7 and -8 along the mouse nephron. Am J Physiol Renal Physiol 2004;286:F1063–1071. [PubMed: 14722018]

Madara JL. Regulation of the movement of solutes across tight junctions. Annu Rev Physiol 1998;60:143–159. [PubMed: 9558458]

Mandell KJ, Parkos CA. The JAM family of proteins. Adv Drug Deliv Rev 2005;57:857–867. [PubMed: 15820556]

Miyamoto T, Morita K, Takemoto D, Takeuchi K, Kitano Y, Miyakawa T, Nakayama K, Okamura Y, Sasaki H, Miyachi Y, Furuse M, Tsukita S. Tight junctions in Schwann cells of peripheral myelinated axons: a lesson from claudin-19-deficient mice. J Cell Biol 2005;169:527–538. [PubMed: 15883201]

Morita K, Furuse M, Fujimoto K, Tsukita S. Claudin multigene family encoding four-transmembrane domain protein components of tight junction strands. Proc Natl Acad Sci U S A 1999;96:511–516. [PubMed: 9892664]

Naderi AS, Reilly RF Jr. Hereditary etiologies of hypomagnesemia. Nat Clin Pract Nephrol 2008;4:80–89. [PubMed: 18227801]

Nitta T, Hata M, Gotoh S, Seo Y, Sasaki H, Hashimoto N, Furuse M, Tsukita S. Size-selective loosening of the blood-brain barrier in claudin-5-deficient mice. J Cell Biol 2003;161:653–660. [PubMed: 12743111]

Piepenhagen PA, Peters LL, Lux SE, Nelson WJ. Differential expression of Na(+)-K(+)-ATPase, ankyrin, fodrin, and E-cadherin along the kidney nephron. Am J Physiol 1995;269:C1417–1432. [PubMed: 8572171]

Reyes JL, Lamas M, Martin D, del Carmen Namorado M, Islas S, Luna J, Tauc M, Gonzalez-Mariscal L. The renal segmental distribution of claudins changes with development. Kidney Int 2002;62:476–487. [PubMed: 12110008]

Riazuddin S, Ahmed ZM, Fanning AS, Lagziel A, Kitajiri S, Ramzan K, Khan SN, Chattaraj P, Friedman PL, Anderson JM, Belyantseva IA, Forge A, Riazuddin S, Friedman TB. Tricellulin is a tight-junction protein necessary for hearing. Am J Hum Genet 2006;79:1040–1051. [PubMed: 17186462]

Ryan A, Dallos P. Effect of absence of cochlear outer hair cells on behavioural auditory threshold. Nature 1975;253:44–46. [PubMed: 1110747]

Salt AN, Melichar I, Thalmann R. Mechanisms of endocochlear potential generation by stria vascularis. Laryngoscope 1987;97:984–991. [PubMed: 3613802]

Simon DB, Lu Y, Choate KA, Velazquez H, Al-Sabban E, Praga M, Casari G, Bettinelli A, Colussi G, Rodriguez-Soriano J, McCredie D, Milford D, Sanjad S, Lifton RP. Paracellin-1, a renal tight junction protein required for paracellular Mg2+ resorption. Science 1999;285:103–106. [PubMed: 10390358]

Tamura A, Kitano Y, Hata M, Katsuno T, Moriwaki K, Sasaki H, Hayashi H, Suzuki Y, Noda T, Furuse M, Tsukita S, Tsukita S. Megaintestine in claudin-15-deficient mice. Gastroenterology 2008;134:523–534. [PubMed: 18242218]

Tsukita S, Furuse M. Pores in the wall: claudins constitute tight junction strands containing aqueous pores. J Cell Biol 2000;149:13–16. [PubMed: 10747082]

Tsukita S, Furuse M. Claudin-based barrier in simple and stratified cellular sheets. Curr Opin Cell Biol 2002;14:531–536. [PubMed: 12231346]

Turksen K, Troy TC. Permeability barrier dysfunction in transgenic mice overexpressing claudin 6. Development 2002;129:1775–1784. [PubMed: 11923212]

Van Itallie CM, Anderson JM. Claudins and epithelial paracellular transport. Annu Rev Physiol 2006;68:403–429. [PubMed: 16460278]

Van Itallie CM, Fanning AS, Anderson JM. Reversal of charge selectivity in cation or anion-selective epithelial lines by expression of different claudins. Am J Physiol Renal Physiol 2003;285:F1078–1084. [PubMed: 13129853]

Wilcox ER, Burton QL, Naz S, Riazuddin S, Smith TN, Ploplis B, Belyantseva I, Ben-Yosef T, Liburd NA, Morell RJ, Kachar B, Wu DK, Griffith AJ, Riazuddin S, Friedman TB. Mutations in the gene encoding tight junction claudin-14 cause autosomal recessive deafness DFNB29. Cell 2001;104:165–172. [PubMed: 11163249]

Yi X, Wang Y, Yu FS. Corneal epithelial tight junctions and their response to lipopolysaccharide challenge. Invest Ophthalmol Vis Sci 2000;41:4093–4100. [PubMed: 11095601]

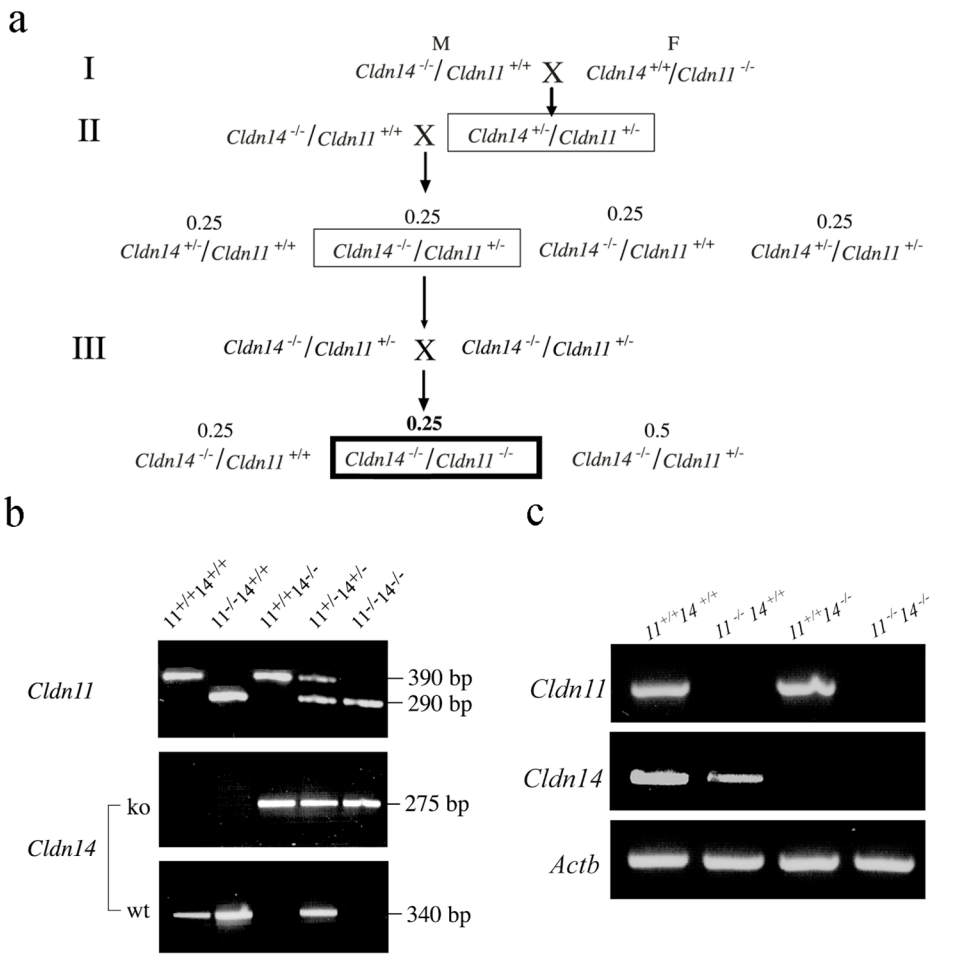

Fig. 1.

Generation of *Cldn11/Cldn14* double knockout mice. **a** Shown are the *Cldn14* and *Cldn11* genotypes of mice used in each set of matings and the genotypes of the offspring. The numbers above the genotypes indicate the proportion of mice with this genotype among all offspring in a given mating. **b** For specific amplification of the wt and the knockout (ko) alleles, if present, from each DNA sample, three different PCR-primers were used in each case (a common primer, a wt primer, and a mutant primer). For *Cldn11* a single multiplexed PCR reaction with all three different PCR-primers is performed. PCR product sizes are 390 bp for the wt allele and 290 bp for the ko allele. For *Cldn14* two separate PCR reactions with two sets of primers (common and wt primers or common and mutant primers) are performed. PCR product sizes are 340 bp for the wt allele and 275 bp for the ko allele. **c** Brain cDNA was analyzed by RT-PCR for *Cldn11* and *Cldn14* expression (512 and 664 bp products, respectively) in mice of various genotypes. As a control, the *Actb* gene (β-actin) (465 bp product) was equally amplified in all samples.

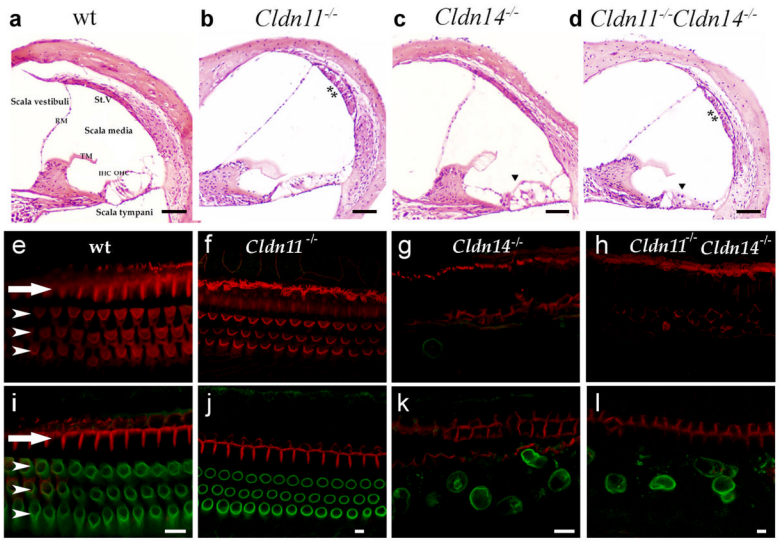

Fig. 2.

Cochlear pathology in *Cldn11*$^{-/-}$, *Cldn14*$^{-/-}$ and *Cldn11*$^{-/-}$/*Cldn14*$^{-/-}$ mice**. a–d** Hematoxylin and eosin staining of paraffin embedded sections (8 μm thick) of the organ of Corti of two months old wt, *Cldn11*$^{-/-}$, *Cldn14*$^{-/-}$ and *Cldn11*$^{-/-}$/*Cldn14*$^{-/-}$ mice (10× magnification). In comparison with the wt mice **(a)**, edema is detected in the St.V of *Cldn11*$^{-/-}$ **(b)** and *Cldn11*$^{-/-}$/*Cldn14*$^{-/-}$ mice **(d)** (asterisks). OHCs of *Cldn14*$^{-/-}$ **(c)** and *Cldn11*$^{-/-}$/*Cldn14*$^{-/-}$ **(d)** mice have degenerated (arrowheads). OHC, outer hair cells; IHC, inner hair cells; TM, tectorial membrane; RM, Reissner's membrane; St.V, stria vascularis. **e-l** Whole mount organ of Corti of wt, *Cldn11*$^{-/-}$, *Cldn14*$^{-/-}$ and *Cldn11*$^{-/-}$/*Cldn14*$^{-/-}$ mice at P16 were processed for immunostaining with an anti-prestin antibody (green), which served as a marker for OHC bodies. Rhodamine-phalloidin staining (red) was used to observe the actin-rich stereocilia and cuticular plate of cochlear hair cells. Shown are confocal cross-sections from the apical region, taken at the level of stereocilia **(e-h)** and the OHC body **(i-l)**. The single row of IHCs is marked by an arrow. The three rows of OHCs are marked by arrowheads. Scale bar = 5 μm.

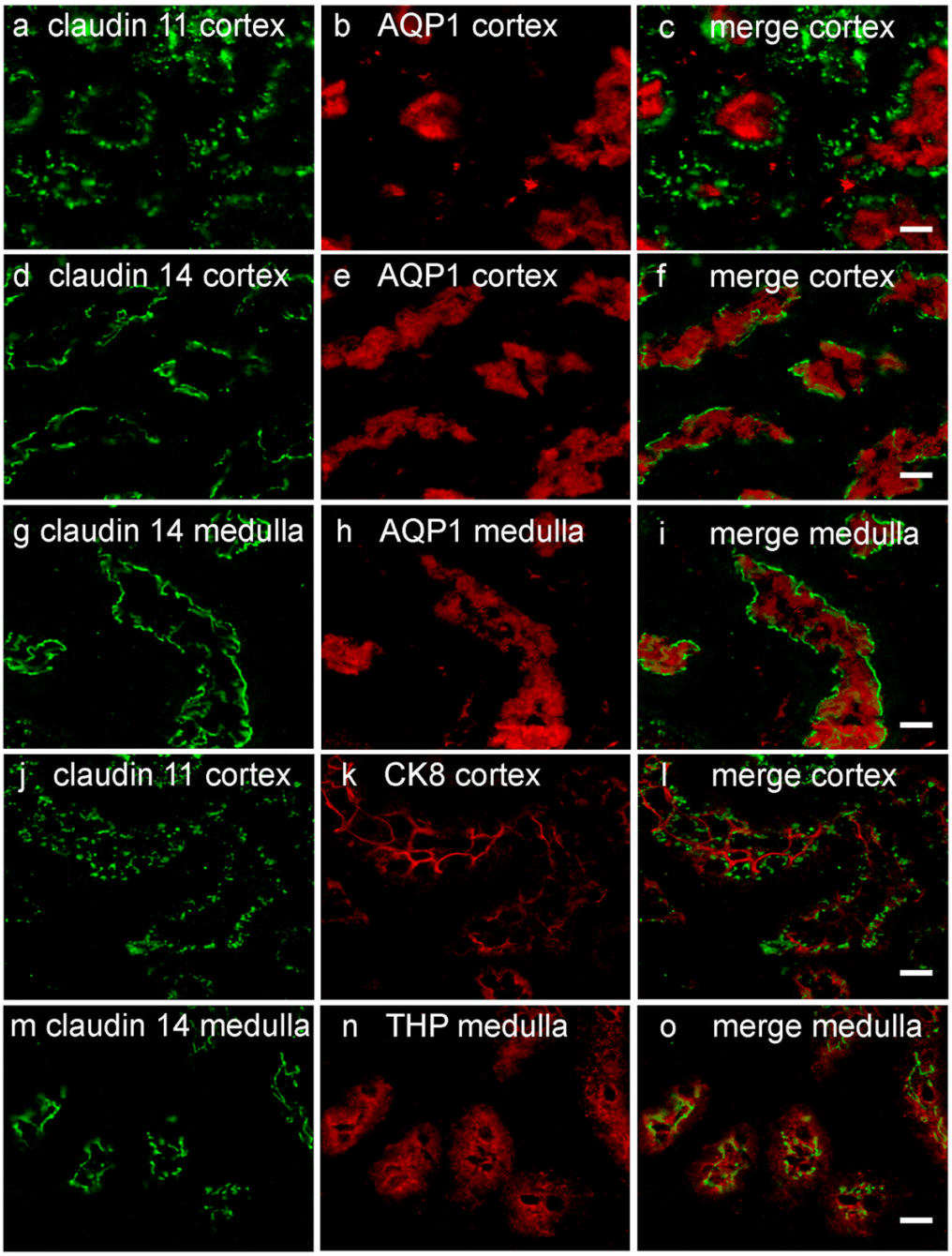

Fig. 3.

Segment-specific expression pattern of claudin 11 and claudin 14 in kidney nephrons. Kidney frozen sections of wt mice at the age of three months were stained with pAb for claudin 11 or claudin 14 (green), and for nephron segment-specific markers (red). Claudin 11 is partially co-localized with AQP1 in the proximal convoluted tubule **(a-c)** and fully co-localized with CK8 in the distal convoluted tubule (cortex) **(j-l)**. Claudin 14 is co-localized with AQP1 in both proximal convoluted tubule (cortex) **(d-f)** and thin descending limb of the loop of Henle (medulla) **(g-i)**, and with THP in the thick ascending limb of the loop of Henle **(m-o)**. Scale bar = 10 μm.

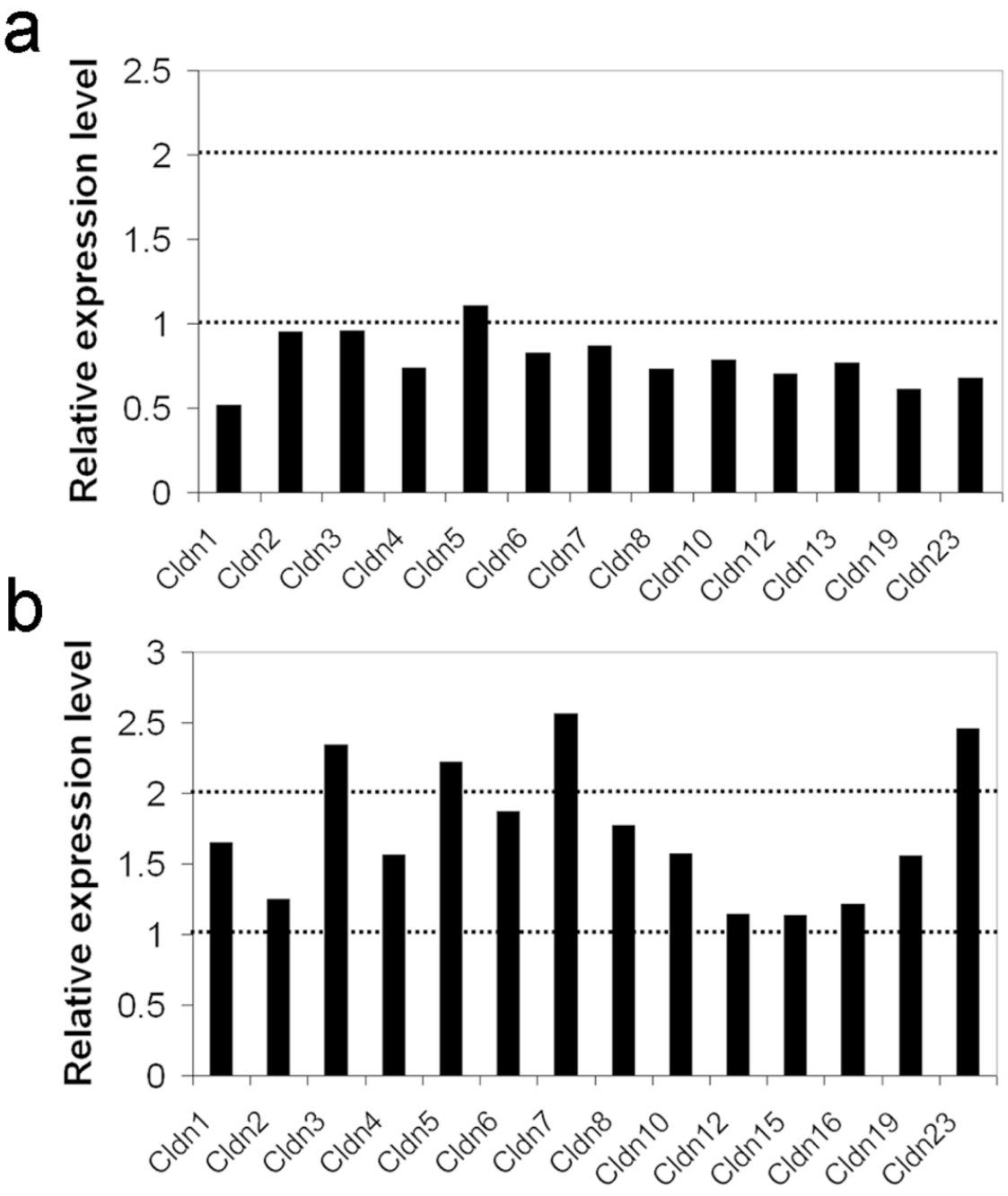

Fig. 4.

Relative expression levels of claudin genes in inner ears **(a)** and kidneys **(b)** of *Cldn11/Cldn14* double knockout mice, as compared to wt mice.

Table 1

Mean ABR thresholds (dB-SPL) of wt, *Cldn11*$^{-/-}$, *Cldn14*$^{-/-}$ and *Cldn11*$^{-/-}$/*Cldn14*$^{-/-}$ mice at the age of two months

Genotype	No of ears analyzed	Frequency (kHz)		
		8	16	32
Cldn11$^{+/+}$*Cld14*$^{+/+}$	8–22	53±8	40±9	52±10
Cldn11$^{-/-}$*Cld14*$^{+/+}$	9–10	80±12	63±13	74±10
Cldn11$^{+/+}$*Cld14*$^{-/-}$	8–10	>97±4	>81±7	81±3
Cldn11$^{-/-}$*Cld14*$^{-/-}$	10	95±5	80±5	75±7

Table 2

Selected renal and systemic characteristics of WT and *Cldn11*$^{-/-}$/*Cldn14*$^{-/-}$ mice

Parameter	WT	$^{-/-}$*Cldn11*$^{-/-}$*Cld14*	P value
P_{Ca++} (mg/dl)	8.92±0.076	8.937±0.139	P=0.9508
U_{Ca++}.V (mg/24h)	0.142±0.017	0.1702±0.025	P=0.3788
P_{Mg++} (mg/dl)	2.097±0.136	2.098±0.085	P=0.9931
U $_{Mg++}$.V (mg/24h)	0.021±0.005	0.036±0.007	P=0.0887
P_{Na+} (mmol/L)	153.43±0.561	152.61±1.555	P=0.6083
U_{Na+}.V (mEq/24h)	179.65±32.868	158.97±22.957	P=0.6246
P_{K+} (mmol/L)	8.58±2.276	7.6±0.717	P=0.7053
U_{K+}.V (mEq/24h)	377.78±48.145	371.76±33.299	P=0.9219
P cr (mg/dl)	0.224±0.089	0.163±0.0115	P=0.5103
Daily urinary volume (ml/24h)	1.425±0.18003	1.2429±0.1601	P=0.4689
GFR (ml/min)	0.174±0.03	0.147±0.018	0.4528
Urinary protein excretion (mg/24h)	5.88±1.1902	4.6028±1.688	P=0.53
Body Weight-BW (g.)	25.625±0.73	25.85±0.553	P=0.8085
Kidney Weight-KW (g.)	0.175±0.0104	0.1627±0.0072	P=0.3672
KW/BW (%)	0.6799±0.028	0.63063±0.0295	P=0.2498
Mean Arterial Pressure (mmHg)	95.34±2.269	91.85±2.43	P=0.3536
Systolic Blood Pressure (mmHg)	114.69±2.416	108.71±2.66	P=0.1185
Diastolic Blood Pressure (mmHg)	85.695±2.75	83.76±3.18	P=0.6531
Heart Rate (beats/min)	390.39±6.81	405.8±6.19	P=0.1164

Values are mean±SEM. n=7 in each group of animals. P_{Ca++}, Plasma Ca^{++} concentration; U_{Ca++}. V, Urinary Ca^{++} excretion; P_{Mg++}, Plasma Mg^{++} concentration; U $_{Mg++}$. V, Urinary Mg^{++} excretion; P_{Na+}, Plasma Na^{+} concentration; U_{Na+}. V, Urinary Na^{+} excretion; P_{K+}, Plasma K^{+} concentration; U_{K+}. V, Urinary K^{+} excretion; P cr, Plasma creatinine concentration; GFR, Glomerular filtration rate.